IMECE2004-59609

RADIAL HEAT TRANSFER DYNAMICS DURING CRYOGEN SPRAY COOLING

Walfre Franco[1,3], **Guo-Xiang Wang**[2], **J. Stuart Nelson**[3] **and Guillermo Aguilar**[1,3*]
[1]Laboratory of Transport Phenomena for Biomedical Applications
Department of Mechanical Engineering, University of California, Riverside, CA 92521
[2]Department of Mechanical Engineering, University of Akron, Akron, OH 44325
[3]Beckman Laser Institute, University of California, Irvine, CA 92612

ABSTRACT

Cryogen spray cooling (CSC) is a heat extraction process that protects the epidermal layer during skin laser surgery of port wine stain (PWS) birthmarks and other specific dermatoses. The objective of the present work is to investigate temporal and radial variations on the heat transferred at the surface of a skin model during CSC. A fast-response thermal sensor is used to measure temperature across the radius of the sprayed surface of a skin model. These interior measurements along with an inverse heat conduction algorithm are used to determine the heat transferred at the surface. Results show that radial and temporal variations of the boundary conditions have a strong influence on the homogeneity of heat extraction from skin. However, there are subregions of uniform cooling. It is also observed that the surface heat flux undergoes a marked dynamic variation, with a maximum heat flux occurring at the center of the sprayed surface early in the spurt followed by a quick decrease. The study shows that external conditions must be taken into account and ideally controlled to guarantee uniform protection during CSC.

INTRODUCTION

Cooling and heating processes are essential to laser surgery for treating specific dermatologic vascular lesions, such as port wine stain (PWS) birthmarks. PWS is a congenital and progressive vascular malformation of the dermis that occurs in approximately 0.7% of children. To remove these birthmarks, laser energy is irradiated at appropriate wavelengths inducing permanent thermal damage to PWS blood vessels. However, laser energy is also absorbed by epidermal melanin causing localized heating therein. As a consequence, complications such as hypertrophic scarring and skin dyspigmentation may occur. Epidermal protection is provided by means of cryogen spray cooling (CSC), which is a spatially selective heat transfer technique that spurts liquid cryogen onto the skin surface. The cryogen evaporates extracting heat from the epidermis thereby increasing the fluence threshold for epidermal damage [1].

The heat extraction from skin during CSC is a function of many fundamental spray parameters that vary in time and space within the spray cone, such as average droplet diameter and velocity, mass flow rate, temperature and spray density [2, 3]. Therefore, the heat extraction process during CSC-assisted skin laser surgery is non uniform [4]. Uniform heat extraction within the sprayed area is highly desirable—to provide homogenous epidermal protection within the laser beam diameter—but not practical, and, despite surface variations, most numerical studies on CSC-assisted skin laser surgery for PWS to date assumed constant heat transfer conditions at the skin surface.

In the present study, surface thermal variations during CSC are experimentally and numerically investigated. A fast-response temperature sensor is used to measure temporal and radial temperature changes along the radius of the sprayed surface of a skin model during CSC. Interior temperature measurements along with an inverse heat conduction problem algorithm are then used to calculate temperatures and heat fluxes at the surface of the skin model.

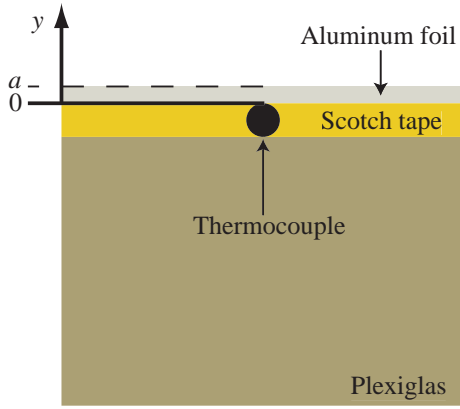*Address all correspondence to this author; email: gaguilar@ucr.engr.edu

Figure 1. FAST-RESPONSE TEMPERATURE SENSOR.

EXPERIMENTAL AND NUMERICAL METHODS

In this section, a brief description of materials and experimental and numerical methods is presented. A more detailed description of the thermal sensor and computer algorithm used herein can be found in the referenced literature.

Cryogen spray cooling system

R-134a, with a boiling temperature at atmospheric pressure of $T_b \approx -26\,°C$, is delivered through a high pressure hose to a fuel injector attached to a straight tube-nozzle. The tube-nozzle has an inner diameter $d = 0.7$ mm and length $l = 32$ mm. All spurts are 60 ms long and the nozzle is positioned at 40 mm from the skin model. The radius of the sprayed surface for this spray system is approximately 9 mm.

Fast-response temperature sensor

The thermal sensor employed is schematically shown in Fig. 1. A miniature type-K thermocouple is placed on top of, 6 mm thick, polymethyl methacrylate (Plexiglas®), and cellulose tape (Scotch tape®), 0.5 mm thick, is placed next to the thermocouple bead to fill the gap between aluminum and skin model. A piece of aluminum foil (15×10 mm and 0.2 mm thick) covers the sensor, and thermal paste around the thermocouple bead is used to ensure good thermal contact. This temperature sensor provides a substrate with thermal properties similar to skin such that their thermal responses are comparable. Thermal properties of human skin, Scotch tape® and Plexiglas® can be found in the literature [5–7]. The initial temperature of the thermal sensor is 22.7 °C.

Initially, the thermocouple bead is placed at the center of the spray cone and, subsequently, displaced away to measure temperatures every 1 mm from the center, $r = 0$ mm, to the periphery of the sprayed surface, $r = 9$ mm. The thermocouple bead is displaced using a BiSlide® (Velmex, Inc.) positioning system, and a new run of spray spurt is applied to measure the temperature history of every location. Repeatability of temperature measurements—shown in the Results and Discussion section—demonstrate that the spray system is very stable, which means that to use only one sensor for all measurements is appropriate.

Inverse heat conduction algorithm

A one-dimensional heat conduction algorithm was used to compute the surface temperature T and heat flux q from the sensor's temperature measurements Y. This approximation relies on the fact that the width of the sprayed area (≈ 18 mm) is much larger than the depth (0.2 mm) of temperature measurements. Indeed, the time scale and depth of relevance in PWS treatment are milliseconds and 0.5 mm, respectively. The solution of a two-dimensional direct heat conduction simulation that justifies the one-dimensional assumption is shown in the next section. The direct problem is solved using a commercial software of finite element method (FEMLAB®).

The applied inverse heat conduction problem algorithm is based on Beck's sequential function specification method (SFSM) [8], where q is estimated as a piecewise constant function of time. The SFSM solves

$$\rho_s c_s \frac{\partial T_s}{\partial t} = k_s \frac{\partial^2 T_s}{\partial y^2} \qquad (1)$$

where ρ, c and k are, respectively, density, specific heat and thermal conductivity, and the subscript s denotes the material—aluminum Al, Scotch tape® or Plexiglas®. The substrate is treated as a semi-infinite body, for which only the following boundary condition at the aluminum surface is needed

$$-k_{Al} \left. \frac{\partial T_{Al}}{\partial y} \right|_{y=a} = q(t), \qquad (2)$$

where a and $q(t)$ are the aluminum foil thickness and the unknown surface heat flux, respectively.

SFSM assumes a functional form of the variation of q over any given discrete time period—the simplest form is a constant q, as used herein. Assuming a constant heat flux q_M^* over a time period t_M to t_{M+1}, Eqs. 1 and 2 are solved for times $t_M, t_{M+1}, \ldots,$ t_{M+r-1} at the corresponding time points and location where temperature was measured during the experiment, i.e., $y = 0$. SFSM uses temperature information of N future time steps. Stable and physically sound results are obtained using multiple future steps, $N \geq 2$. In this study 5 future steps are used to calculate surface heat fluxes. It follows that the actual surface heat flux q_M can be calculated from the assumed heat flux q_M^* as

$$q_M = q_M^* + \frac{\sum_{n=1}^{N} (Y_{M+n-1} - T_{M+n-1}^*) Z_{n-1}}{\sum_{n=1}^{N} (Z_{n-1})^2}, \qquad (3)$$

2

where Z_n is the sensitivity coefficient defined at $y = 0$ as

$$Z_n = \frac{\partial T_n}{\partial q_M}. \qquad (4)$$

The sensitivity coefficient can be obtained by solving Eq. 1 under the same geometry with T replaced by Z and boundary condition

$$-k_{Al} \left. \frac{\partial Z_n}{\partial y} \right|_{y=a} = 1. \qquad (5)$$

A discussion of this algorithm as applied to CSC can be found elsewhere [9].

RESULTS AND DISCUSSION

The repeatability of experiments and verification of the one-dimensional approximation are presented in Fig. 2. The average values $\overline{T}$ of four independent temperature measurements at the center of the sprayed area are shown in Fig. 2(a), the error bars denote standard deviations. Similar curves were obtained for the remaining locations. Isotherms within a Plexiglas substrate and aluminum foil cover are presented in Fig. 2(b). Isotherms within the aluminum foil are straight vertical lines, which means that the temperature gradient in the radial direction is negligible within the scale of the thermocouple bead size, and, for this reason, one dimensional. Curves correspond to the solution of a two-dimensional heat diffusion simulation for which dynamic and radial experimental measurements of surface temperature—presented in next section—are used as boundary condition.

Heat transfer dynamics

Dynamics of surface temperature T for every measurement location are shown in Fig. 3(a). The vertical and horizontal dashed lines denote the end of the 60 ms cryogen spurt and cryogen boiling temperature, respectively. The closer the thermocouple bead is to the center of the spray cone, the lower the minimum T and the longer it takes to reach this local minimum. Also, the slopes of curves during the cryogen spurt illustrate that locations closer to the center undergo a higher rate of change of T, thus the heat extraction process is faster. A separation of curves is evident during and after the spurt: there is a set of locations that show similar $T(t)$ values, this set corresponds to the grouped curves at the bottom of Fig. 3(a). It follows that there are regions of uniform radial cooling.

Dynamics of surface heat flux q for every measurement location are shown in Fig. 3(b). The dashed line denotes the end of the 60 ms cryogen spurt. The closer the thermocouple bead is to the center of the spray cone, the higher the q. This is true
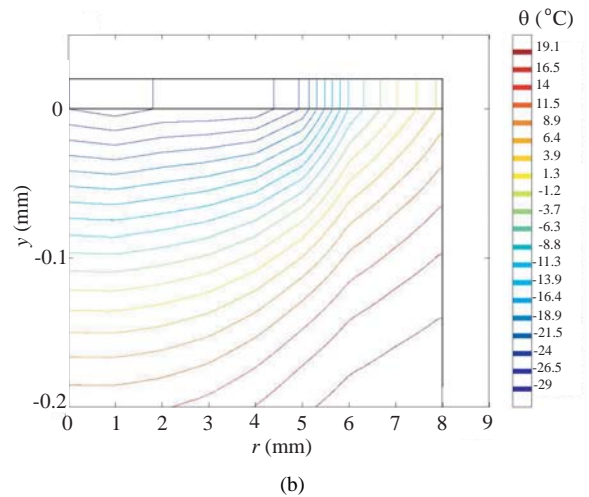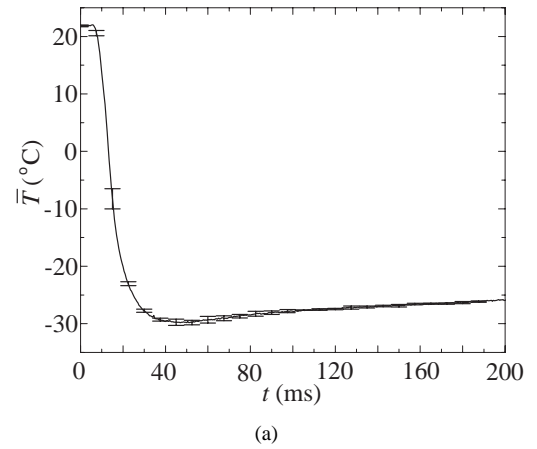

(a)

(b)

Figure 2. (a) AVERAGE TEMPERATURES FOR $r = 0$ mm. BARS DENOTE STANDARD DEVIATIONS. (b) ISOTHERMS WITHIN ALUMINUM AND PLEXIGLAS AT $t = 100$ ms.

before the central locations reach local maximum values. By inspecting curve slopes during the first time instants, it can be seen that closer to the center the q rate of change is higher. Note that maximum curve values occur at different times, the closer to the center the earlier in time the local maximal heat flux q_{max} occurs. Table 1 shows values of q_{max} and correspondent times for each measurement location. q_{max} at every location occurs before the cryogen spurt ends. The difference in time between the first and last q_{max} is as large as 50 ms. The small fluctuations in time of surface heat flux are artifacts from the heat flux estimation procedure.

Differences in temperature ΔT_i and heat flux Δq_i are used to assess how uniform cooling conditions at the surface are both, radially and temporary. ΔT_i is defined as the difference in temperature value among the center of the sprayed area and measurement

3
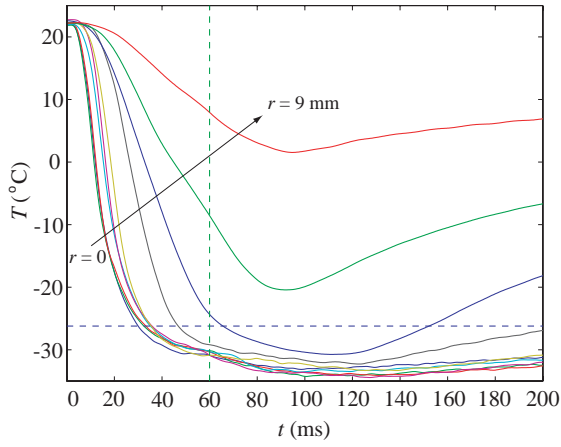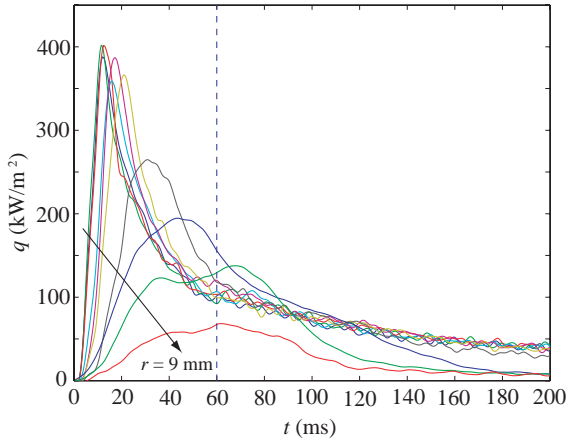
Figure 3. DYNAMICS OF (a) TEMPERATURE AND (b) HEAT FLUX AT SURFACE. VERTICAL AND HORIZONTAL DASHED LINES DENOTE END OF CRYOGEN SPURT AND CRYOGEN BOILING TEMPERATURE, RESPECTIVELY.

Table 1. LOCAL MAXIMUM HEAT FLUXES.

r (mm)	t (ms)	q_{max} (kW/m^2)
0	12.0	387.8
1	11.5	401.9
2	12.5	401.7
3	16.0	359.0
4	17.0	386.9
5	21.0	366.5
6	31.0	264.8
7	43.5	194.6
8	68.0	137.6
9	61.5	68.3

location i, that is

$$\Delta T_i = T(t, r_0) - T(t, r_i), \qquad (6)$$

where $i = 1, 2, ..., 10$. The measurement locations are $r_0 = 0$, $r_1 = 1$, $r_2 = 2$, ..., and $r_9 = 9$ mm. Similarly, the difference in heat flux Δq_i is defined as

$$\Delta q_i = q(t, r_0) - q(t, r_i). \qquad (7)$$

Temporal variations of ΔT for every location are shown in Fig. 4(a). The dashed line denotes the end of the 60 ms cryogen spurt. As time goes by, temperature differences respect to the center of the sprayed area become larger. Among the center and the periphery, ΔT_9, the difference is more than 35 °C by the end of the cryogen spurt, $t = 60$ ms. Temporal variations of Δq for every location are shown in Fig. 4(b). The dashed line denotes the end of the cryogen spurt. There are also large differences in heat flux among central and peripheral locations. At certain times, Δq is negative, hence the heat extraction is higher at middle locations than at those by the center and periphery.

### Radial heat transfer dynamics

Radial distributions of T for different times are shown in Fig. 5(a). Curves are shown in 15 ms intervals. Initially, every location is at room temperature, $T = 22.7$ °C (first curve from top to bottom). Next, the cryogen liquid cools down the skin model and temperature at every location decreases at different rates. The fifth curve from top to bottom corresponds to the end of the spurt.

Radial distributions of q at 15 ms intervals are shown in Fig. 5(b). At $t = 0$ ms the skin model is in thermal equilibrium. Next, the cryogen liquid extracts heat from the skin model and a heat flux from the model to the surrounding environment establishes. The curve with the largest values corresponds to 15 ms. q undergoes a marked dynamic variation, with maximum heat fluxes occurring at the center of the sprayed surface early in the spurt followed by a quick decrease.

As shown, cooling is not uniform neither in time nor in space. However, Fig. 5(a) and 5(b) illustrate that there are subregions within the sprayed surface where surface cooling conditions are homogeneous. These subregions are defined by the radius and times for which temperature and heat flux values among locations are similar. The radius and times of these subregions
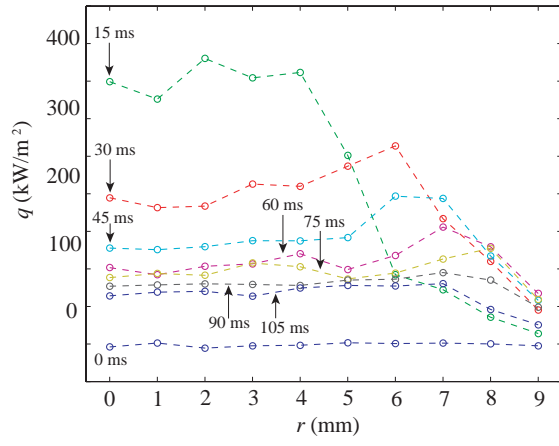
4
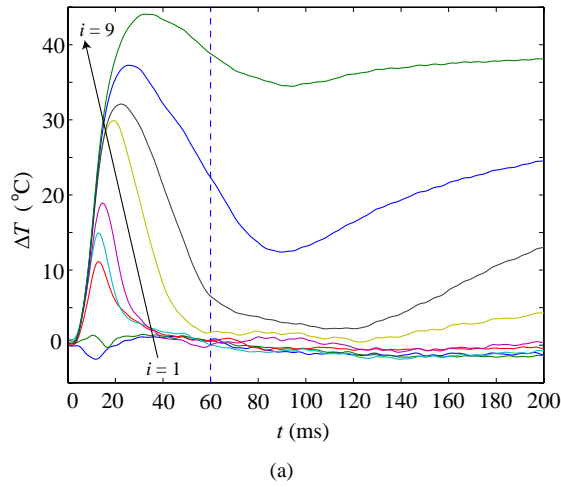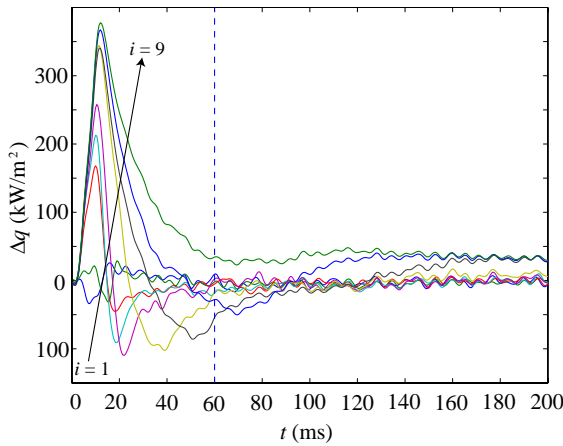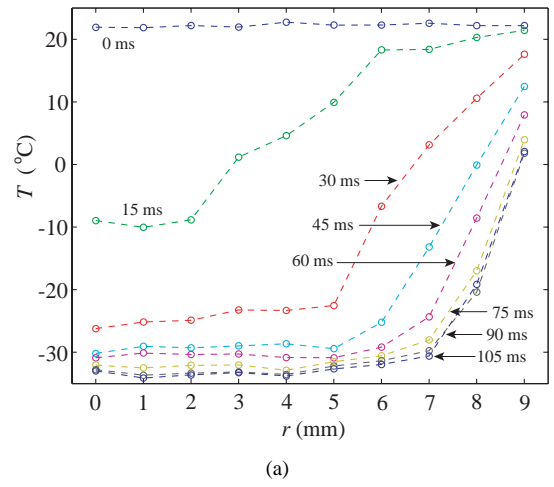
Figure 4. DYNAMICS OF DIFFERENCES IN (a) TEMPERATURE AND (b) HEAT FLUX AMONG CENTER AND REST OF LOCATIONS. DASHED LINE DENOTES ENF OF CRYOGEN SPURT.
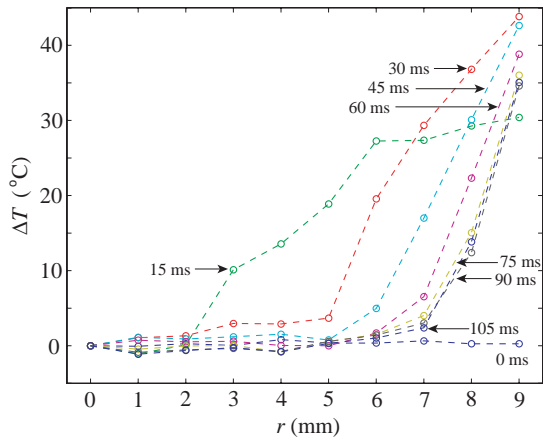

Figure 5. RADIAL DISTRIBUTIONS OF (a) TEMPERATURE AND (b) HEAT FLUX AT SURFACE.

are shown in Fig. 6(a) and 6(b). For the spray system studied herein, cooling conditions are uniform within a 2 mm radius at any time, and for $t \geq 60$ ms, surface conditions are uniform radially within a 7 mm radius.

Discussion

Fluid mechanics and heat transfer of spray systems are highly complex. Cooling conditions at the skin boundary vary radially and temporary during CSC and afterward. Therefore, the epidermal protection provided is non-uniform. However, Fig. 4 and 6 show that there are subregions where cooling conditions are homogeneous within the spray cone, hence subregions of uniform epidermal protection can be identified, provided that the laser beam radius is smaller or equal to the subregion radius. The radius of uniform protection area is time dependent, conse-

quently the instant at which the laser pulse is supplied is critical as it is illustrated next. Surface temperature values are similar at 105 ms, Fig. 4(a), in a 7 mm radius, Fig. 6(a). Nevertheless CSC is intended to be a selective heat extraction process. It is possible that at 105 ms the temperature of the targeted PWS blood vessels could be reduced unintentionally. It follows that more energy will be needed to reach the threshold damage of the blood vessels. In CSC-assisted skin laser surgery, the laser pulse is supplied either at the end of the cryogen spurt or 30 to 40 ms after. The region of uniform epidermal protection within these time frames has an approximate radius of 7 mm. A laser beam with a radius equal to or less than 7 mm would be appropriate. As the radius of the laser beam increases, chances of epidermal damage at the perimeter of the beam increase as well. Consequently, there is a critical relation among laser beam radius and subregions of uniform cooling, and external conditions must be

5
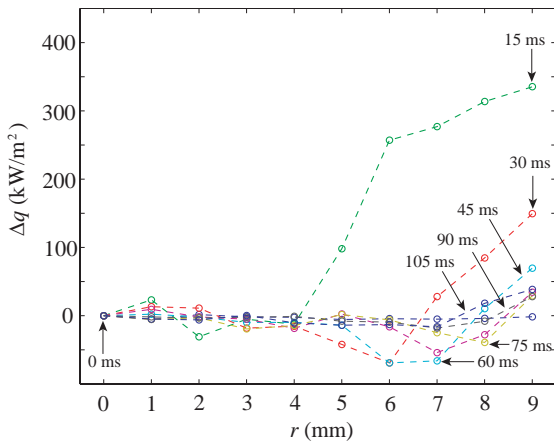
Figure 6. RADIAL DISTRIBUTION OF DIFFERENCES IN (a) TEMPERATURE AND (b) HEAT FLUX AMONG CENTER AND REST OF LOCATIONS.

taken into account and ideally controlled to guarantee uniform skin protection during CSC.

CONCLUSIONS

A fast-response temperature sensor was used to study radial heat transfer dynamics on a skin model during CSC. The sensor was used to collect temperature data every 1 mm on a 9 mm radius from the center of the sprayed surface to the periphery. The heat transfer process at the surface is a complex temporal and spatial phenomenon. The difference in temperatures among different locations is significant, especially between central and peripheral locations. Closer to the center, the dynamic thermal response is faster and lower temperatures are reached. The overall maximum heat flux q_{max} takes place early in time at the center

of the sprayed surface. For $r = 2$ mm the temperature differences among the center and locations within this area are less than 5 °C at any time. Epidermal protection provided by CSC is not uniform. However, there exist subregions of uniform cooling conditions within the sprayed area and consequently subregions of uniform epidermal protection. Therefore, skin boundary conditions must be taken into account and controlled in order to guarantee uniform epidermal protection during CSC-assisted skin laser surgery.

ACKNOWLEDGMENT

REFERENCES

[1] Nelson, J. S., Milner, T. E., Anvari, B., Tanenbaum, B. S., Kimel, S., Svaasand, L. O., and Jacques, S. L., 1995. "Dynamic epidermal cooling during pulsed-laser treatment of port-wine stain - a new methodology with preliminary clinical-evaluation". Arch. Dermatol., **131** (6) , pp. 695–700.

[2] Aguilar, G., Majaron, B., Pope, K., Svaasand, L. O., Lavernia, E. J., and Nelson, J. S., 2001. "Influence of nozzle-to-skin distance in cryogen spray cooling for dermatologic laser surgery". Lasers Surg. Med., **28** (2) , pp. 113–120.

[3] Karapetian, E., 2002. Influence of cryogenic spray parameters on surface heat extraction on human skin. Master's thesis, Department of Chemical Engineering and Materials Science, University of California, Irvine, California.

[4] Franco, W., Wang, G. X., Karapetian, E., JS, J. S. N., and Aguilar, G., 2004. "Effect of surface thermal variations during cryogen spray cooling in dermatologic laser therapy". In Proc. ILASS Americas. 17th Annual Conference on Liquid Atomization and Spray Systems.

[5] Aguilar, G., Wang, G. X., and Nelson, J. S., 2003. "Effect of spurt duration on the heat transfer dynamics during cryogen spray cooling". Phys. Med. Biol., **48** (14) , pp. 2169–2181.

[6] Aguilar, G., Diaz, S. H., Lavernia, E. J., and Nelson, J. S., 2002. "Cryogen spray cooling efficiency: Improvement of port wine stain laser therapy through muttiple-intermittent". Lasers Surg. Med., **31** (7) , pp. 27–35.

[7] Duck, F. A., 1990. *Physical properties of tissue*. Academic press, London.

[8] Beck, J. V., Blackwell, B., and St. Clair, Jr., J. R., 1985. *Inverse heat conduction: ill posed problems*. Wiley, New York.

[9] Tunnel, J. W., Torres, J. H., and Anvari, B., 2002. "Methodology for estimation of time-dependent surface heat flux due to cryogen spray cooling". *Ann. Biomed. Eng.,* **30** , pp. 19–33.